Scripta Materialia 206 (2022) 114231

Contents lists available at ScienceDirect

Scripta Materialia

journal homepage: www.elsevier.com/locate/scriptamat

The cross-transition of deformation twinning in magnesium

Nan Yang, Bo-Yu Liu*, Fei Liu, Zhi-Wei Shan*

Center for Advancing Materials Performance from the Nanoscale (CAMP-Nano) & Hysitron Applied Research Center in China (HARCC), State Key Laboratory for Mechanical Behavior of Materials, Xi'an Jiaotong University, Xi'an 710049, PR China

ARTICLE INFO

Article history:
Received 15 June 2021
Revised 18 August 2021
Accepted 22 August 2021

Keywords:
Magnesium
Twinning
Interface migration
Plastic deformation
TEM

ABSTRACT

Deformation twinning operates *via* twinning dislocations gliding on a specific twinning plane and along a specific twinning direction. As a consequence, a twin variant is supposed to retain its identity and unable to transform into other variants. However, we demonstrated that for the $\{10\bar{1}2\}$ deformation twinning in magnesium, one twin variant can transform towards its conjugated variant in response to the external applied loading *via* the participation of prismatic-basal interface migration. We term such transformation as cross-transition of deformation twinning, which is expected to broaden the understanding of twinning mechanism.

According to classic twinning theory, deformation twinning (DT) operates *via* twinning dislocations successively gliding on atomically adjacent twinning planes, and shears the material along a certain twinning direction and twinning plane [1–5]. Given a certain twin variant, it usually develops into a straight lamella with its boundary, *i.e.* the twin boundary (TB), generally parallel to the twinning plane, and cannot transform into other twin variants. The straight TBs that are strictly parallel to the twinning plane are widely observed in metals with face-centered cubic structure [6–9]. However, for the $\{10\bar{1}2\}$ DT, a very common DT mode in hexagonal close-packed (hcp) metals, its TB usually exhibits irregular morphology, which means that $\{10\bar{1}2\}$ TB is not necessarily parallel to twinning plane [10–19]. Detailed characterization shows that the irregular $\{10\bar{1}2\}$ TB is usually composed of $\{10\bar{1}2\}$ coherent twin boundary (CTB) and basal/prismatic (BP) interfaces [13–17,19]. In the past few years, there have been many efforts to study the mechanism of $\{10\bar{1}2\}$ DT and to explain the unusual twinning behaviors, but a consensus has not emerged [20].

The BP interfaces migrate *via* basal-prismatic transformation, which was called as unit-cell-reconstruction (UCR) by Liu et al. [13]. Since the UCR can result in a $\{10\bar{1}2\}$ twinning-like 90° of orientation relationship, here we use the term "90° twin" to refer the resulted lattice by UCR. As shown in Fig. 1a, the consequence by UCR can be regarded as that the matrix (blue) rotates 90° around $[\bar{1}2\bar{1}0]$ to become the "90° twin" lattice (red). The $(10\bar{1}2)$ twin variant has mirror symmetry with matrix about the $(10\bar{1}2)$ CTB, which is equivalent to a 93.7° rotation around $[\bar{1}2\bar{1}0]$. Thus, the orientation difference between $(10\bar{1}2)$ twin and "90° twin" by UCR is a 3.7° rightward rotation. Similarly, the orientation difference between $(\bar{1}012)$ twin and "90° twin" is a 3.7° leftward rotation. Such 3.7° of difference between $\{10\bar{1}2\}$ twin and "90 ° twin" is small and thus can be accommodated elastically, which allows the coexistence of $\{10\bar{1}2\}$ CTB and BP interfaces [21,22]. Furthermore, molecular dynamics simulations show that both $(10\bar{1}2)$ and $(\bar{1}012)$ CTBs can simultaneously develop from a single BP segment and coexist on the boundary [13,23]. One typical result is shown in Fig. 1b. This suggests that BP interface can serve as a bridge to connect conjugated $\{10\bar{1}2\}$ TBs. Inspired by such phenomenon, we propose that one $\{10\bar{1}2\}$ TB can transform into its conjugate counterpart, *i.e.* TB→BP→$\text{TB}_{\text{conjugate}}$. As a result, one $\{10\bar{1}2\}$ twin variant can probably evolve into its conjugated variant. Such twin→$\text{twin}_{\text{conjugate}}$ transition is termed as cross-transition of DT.

Considering that the orientation difference between $(10\bar{1}2)$ and $(\bar{1}012)$ twin variants is only 7.4° (7.4° = 93.7°–86.3° = 2 × 3.7°), we expect that the cross-transition of $\{10\bar{1}2\}$ DT can occur by rotating the twin volume, as illustrated in Fig. 2. A $(10\bar{1}2)$ twin exists in a pillar with its axis along $[10\bar{1}0]_{matrix}$, the twin volume tilt rightward by 3.7° due to the twinning shear (Fig. 2a). The twin-induced tilt will cause a lateral shift of the pillar top, $D^{\parallel}_{top}$. If this pillar is subjected to an external applied loading that tilts the pillar to right (*e.g.* a compression with its loading direction not exactly parallel to the pillar axis but pointing to the lower right), consistent with the tilt direction produced by the initial $(10\bar{1}2)$ twin, then this twin is expected to grow in a normal way, *i.e.* the $(10\bar{1}2)$ CTB moves forward without changing its shape (Fig. 2b–d). Instead, if the applied loading tilts the pillar to left, in the same

* Corresponding authors.
E-mail addresses: boyuliu@xjtu.edu.cn (B.-Y. Liu), zwshan@mail.xjtu.edu.cn (Z.-W. Shan).

https://doi.org/10.1016/j.scriptamat.2021.114231
1359-6462/

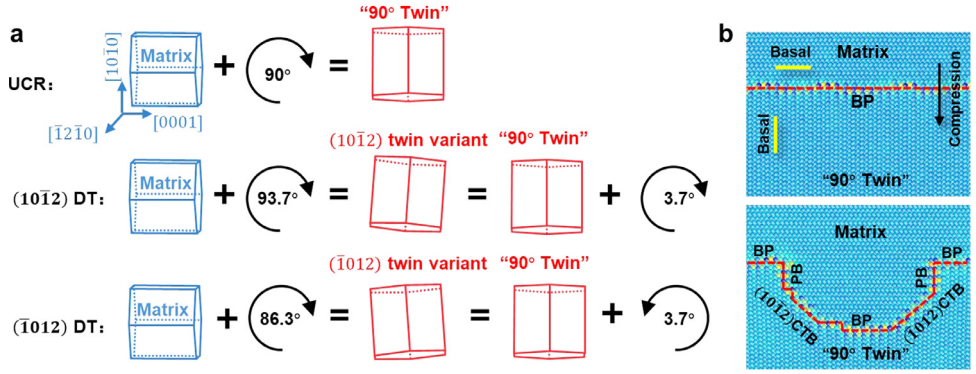

Fig. 1. (a) Schematics illustrating the resultant lattice orientation by UCR, (10$\bar{1}$2) and ($\bar{1}$012) DT. (b) MD simulation result showing both (10$\bar{1}$2) and ($\bar{1}$012) CTBs can simultaneously develop from a single BP segment [13] (For interpretation of the references to color in this figure, the reader is referred to the web version of this article).

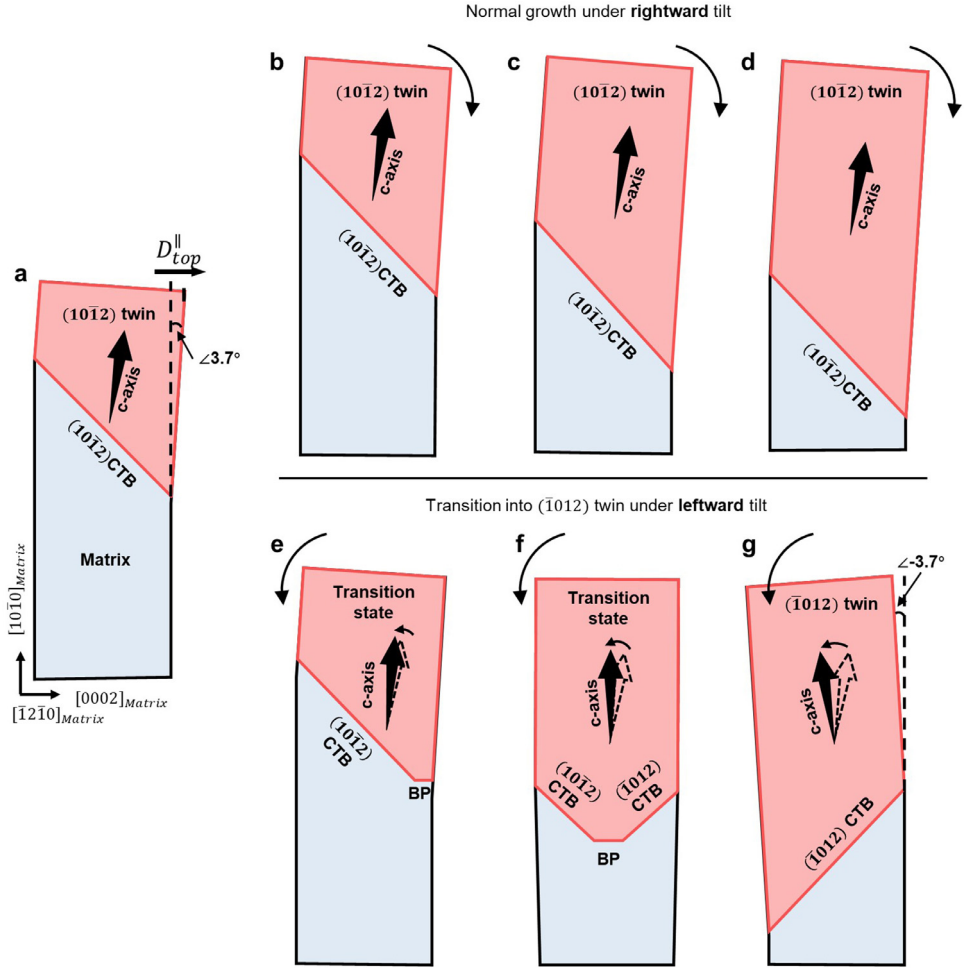

Fig. 2. Schematics illustrating the normal growth and cross-transition of {10$\bar{1}$2} DT. (a) Initial bicrystal containing a (10$\bar{1}$2) twin variant. The bold arrow indicates the c-axis of the twin. (b–d) The normal growth of (10$\bar{1}$2) twin under an applied loading that tilt the pillar to right. (e–g) Transition from (10$\bar{1}$2) twin to ($\bar{1}$012) twin under an applied loading that tilts the pillar to left.

direction with the tilt produced by ($\bar{1}$012) twin variant, then the initial (10$\bar{1}$2) twin is expected to transform into ($\bar{1}$012) twin to accommodate the applied loading. If (10$\bar{1}$2) twin directly transforms into ($\bar{1}$012) twin, this process is equivalent to rotate the twin by 2 × 3.7° in one step. However, if the (10$\bar{1}$2) twin first becomes "90° twin" (rotating 3.7°), then becomes ($\bar{1}$012) twin (rotating another 3.7°), this transformation can thus be accomplished by two easier steps. Therefore, we surmise that the cross-transition should be operated with the assistance of a BP interface as an intermediate, *i.e.* (10$\bar{1}$2) CTB→BP→($\bar{1}$012) CTB. As can be seen from Fig. 2e–g, once BP and ($\bar{1}$012) CTB form, the pillar will tilt left and the orientation of the whole twin volume will deviate from the initial orientation of (10$\bar{1}$2) twin variant. We refer this stage as a transition stage. After the whole twin becomes ($\bar{1}$012) variant, the pillar will tilt leftward for 3.7° and the cross-transition is completed.

A group of *in-situ* transmission electron microscope (TEM) compression tests on submicron magnesium single crystal pillars are performed to verify the occurrence of cross-transition. The pillars are compressed by a diamond punch and the pillar length

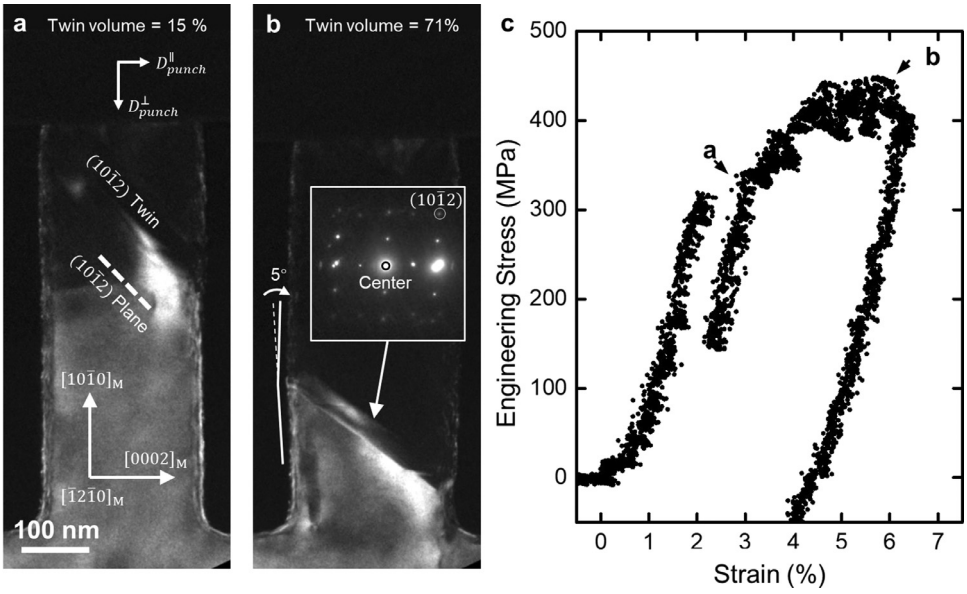

Fig. 3. A $(10\bar{1}2)$ TB normally migrates when $D^{\parallel}_{punch}$ is in the same direction of the $D^{\parallel}_{top}$ (positive). (a) and (b) Snapshots captured from *in-situ* movie showing the migration of a $(10\bar{1}2)$ TB. $\vec{g}$ is $(10\bar{1}1)_{matrix}$. Viewing direction, $\sim[1\bar{2}10]$. Inset in (b) is the SAED captured at the TB. The pillar's left surface in (b) is depicted by a white kinked line. (c) The corresponding engineering stress-strain curve. The positions corresponding to (a) and (b) are arrowed on the curve.

direction is set to $\sim[10\bar{1}0]$. Compression along $\sim[10\bar{1}0]$ in magnesium will activate $\{10\bar{1}2\}$ DT [24]. The Schmid factors for the $(10\bar{1}2)$ and $(\bar{1}012)$ twin variants in each pillar are listed in Table S1. The *in-situ* experiments are monitored under a view direction along $[\bar{1}2\bar{1}0]$. Sample preparation method can be found in our previous works [13,25]. Before compression, we purposely moved the punch laterally with large steps and quick speed by piezo control. This makes the punch keep moving laterally during compressive loading (can be regarded as "inertia" effect of the punch). As a result, a non-uniaxial compression with both lateral and vertical displacement of the punch ($D^{\parallel}_{punch}$ and $D^{\perp}_{punch}$) can be performed on the pillar, which will tilt the pillar along the direction of $D^{\parallel}_{punch}$. The movement trace of the punch is shown by tracking a marker on the punch (Supplementary Movies 1 and 2). The sign of $D^{\parallel}_{punch}$ is designated as positive or negative when it is in the same or opposite direction to the twin-induced $D^{\parallel}_{top}$, respectively. When the $D^{\parallel}_{punch}$ is positive, the loading will tilt the pillar to a direction in consistent with the existed $\{10\bar{1}2\}$ twin and the TB can normally migrate, similar to the situation of Fig. 2b–d. Instead, if the $D^{\parallel}_{punch}$ is negative, the loading will tilt the pillar to a direction in consistent with the conjugated twin, then cross-transition is expected to occur, similar to the condition of Fig. 2e–g. Fifteen tests were conducted. The results can be classified into two groups. For the 8 tests with positive $D^{\parallel}_{punch}$, the TB normally migrates with no cross-transition occurs; while in the rest 7 tests with negative $D^{\parallel}_{punch}$, cross-transition occurs, as summarized in Figs. S1 and S2.

A typical example of TB normal migration is demonstrated in Fig. 3 and Supplementary Movie 1. In this test, the $D^{\parallel}_{punch}$ is along $[0002]_{matrix}$ (towards right in the figure). A $(10\bar{1}2)$ twin formed in top part of the pillar after the stress reached ~320 MPa (Fig. 3a), corresponding to the strain burst and stress drop on the stress-strain curve (Fig. 3c). This $(10\bar{1}2)$ twin caused a rightward $D^{\parallel}_{top}$, in the same direction of the $D^{\parallel}_{punch}$ (positive). During further compression, the twin grew *via* the downwards migration of the lower TB (Fig. 3b). When the TB reached the root part of the pillar, we retreated the punch. Interestingly, we found that detwinning occurred during unloading even when the flow stress was not down to zero (Supplementary Movie 1). When the TB migrated backwards, no dislocation was observed neither in the twin nor in the matrix. A possible reason for such detwinning is the elastic back stress resulted by the geometrical constraint of pillar root. During the entire testing, this TB was almost parallel to $(10\bar{1}2)$ with no obvious change of boundary shape and orientation. Selected area electron diffraction (SAED) pattern acquired at the TB shows that the $(10\bar{1}2)$ spots of twin and matrix are overlapped, indicating a $(10\bar{1}2)$ twin relation and this TB is thus a $(10\bar{1}2)$ TB. The shear strain produced by this $(10\bar{1}2)$ twin variant caused a right tilt of the twinned volume with respect to the un-twinned volume. This can be reflected by the ~5° angle between the left surface of the twin and matrix, as marked by the kinked line in Fig. 3b.

A typical example of cross-transition is demonstrated in Fig. 4 and Supplementary Movie 2. In this test, the $D^{\parallel}_{punch}$ is along $[000\bar{2}]_{matrix}$ (towards left in the figure). During compression, a $(10\bar{1}2)$ twin formed in top part of the pillar when the stress reached ~350 MPa (Fig. 4a). Similarly, strain burst and stress drop corresponding to the twin formation (Fig. 4e). Note that this $(10\bar{1}2)$ twin should cause a rightward $D^{\parallel}_{top}$, in the opposite direction of the $D^{\parallel}_{punch}$ (negative). The $(10\bar{1}2)$ TB first normally migrated downwards (Fig. 4b). When the TB reached the middle part of pillar, a segment of TB along $(\bar{1}012)$ appeared at the right end of the TB (Fig. 4c). From this moment on, the twinned volume starts to tilt leftwards (Supplementary Movie 2). At the same time, the corresponding flow stress suddenly increased to ~410 MPa (Fig. 4e). As shown in the inset of Fig. 4c, the arrangement of the two TBs gave rise to a *V*-shaped morphology. Note that the tip of the *V*-shaped TB (*V*-tip) is blunt as outlined by the red dashed line in the inset. Such blunt segment should be composed by BP interfaces, which bridges the left and right TB segment. Then, the right TB segment gradually elongated during continuous loading, leading to the left movement of the *V*-tip. In Fig. 4d, the *V*-tip fast moved to the central axis of the pillar, corresponding to a load drop. Since twin nucleation can also lead to load drop, we carefully analyzed the *in-situ* movie and postmortem characterizations to confirm that no new twin formed. In this compression test, only part of the $(10\bar{1}2)$ TB has transited into $(\bar{1}012)$ TB, therefore the twin should

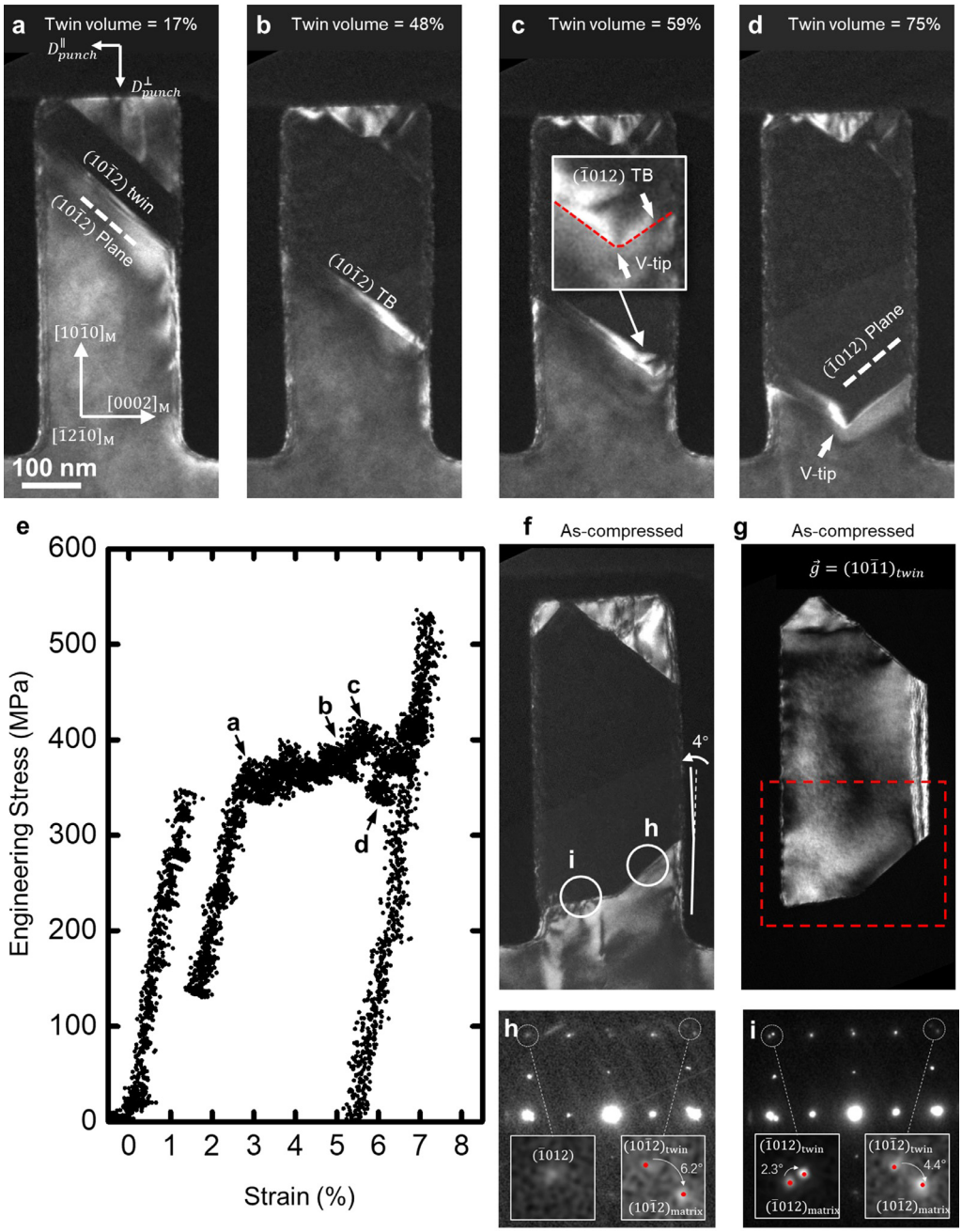

Fig. 4. Cross-transition of DT when $D^{\parallel}_{punch}$ is in the opposite direction of the $D^{\parallel}_{top}$ (negative). (a–d) Snapshots captured from the *in-situ* movie. (a) Twin formation. The trace of $(10\bar{1}2)$ is marked by a white dashed line. (b) TB normally migrates. (c) Formation of a $(\bar{1}012)$ boundary segment, causing a *V*-shaped TB (inset is an enlarged view). (d) Elongation of the $(\bar{1}012)$ boundary segment. The trace of $(\bar{1}012)$ is marked by a white dashed line. (e) Corresponding engineering stress-strain curve. The positions corresponding to (a) to (d) are arrowed on the curve. (f) and (g) Dark-field images of the as-compressed pillar with the matrix and twin in bright contrast, respectively. The right surface of the pillar in (f) is depicted by a white kinked line. (h) and (i) SEAD captured at the right and left segment of TB in (f). Insets are the enlarged views of circled area. $\vec{g}$ vector for (a–d) and (f), $(10\bar{1}1)_{matrix}$, for (g), $(10\bar{1}1)_{twin}$. Viewing direction, ~$[1\bar{2}10]$ (For interpretation of the references to color in this figure, the reader is referred to the web version of this article).

be in a transition state as referred in Fig. 2f. After the TB migrated to the root part of the pillar, we continuously compressed the pillar, which led to a dramatic increase of flow stress (Fig. 4e), and the left part of the *V*-shaped TB (the $(10\bar{1}2)$ segment) deviated from $(10\bar{1}2)$ plane and become horizontal. The loading was then retreated.

To ascertain the identity of the as-transited twin, we characterized the as-deformed pillar (Fig. 4f and 4g). The right part of the lower TB is almost parallel to $(\bar{1}012)$ plane and the left part is approximately parallel to the $(10\bar{1}0)_{matrix}$. SAED pattern acquired at right TB shows that the $(\bar{1}012)$ spots of twin and matrix are overlapped (Fig. 4h), indicating a $(\bar{1}012)$ twin relation. Therefore, the right TB segment should be a $(\bar{1}012)$ TB. The SAED pattern acquired at the left TB shows a split of both $(10\bar{1}2)$ spots and $(\bar{1}012)$ spots (Fig. 4i), indicating that BP interfaces dominate the left segment of TB [13]. There is almost no dislocation in the twin volume, as well as in the place near the lower TB (marked by the red dashed box of Fig. 4g). The twin tilts left by ~ 4° with respect to the matrix, as reflected by the kinked line in Fig. 4f. Based on the above evidences, we identify that cross-transition occurred, despite the initial $(10\bar{1}2)$ TB hasn't completely transformed into $(\bar{1}012)$ TB.

To recap, we experimentally demonstrated that the cross-transition of $\{10\bar{1}2\}$ DT can occur when the loading tilts initial $(10\bar{1}2)$ twin to a direction in consistent with the conjugated $(\bar{1}012)$ twin. The cross-transition is a progressive and continuous process achieved by the generation and elongation of $(\bar{1}012)$ TB from the initial $(10\bar{1}2)$ TB, as well as the simultaneously rotation of the twinned volume. During the cross-transition, two conjugated $\{10\bar{1}2\}$ CTBs and BP interfaces coexist on a single TB. In our observation, there are no dislocations near the TB, which implies the orientation differences across the conjugated $\{10\bar{1}2\}$ CTBs and BP interfaces should be accommodated elastically. For a submicron pillar, such elastic strain can be released by the free surface since the pillar's specific surface area is large. As the elongation of $(\bar{1}012)$ TB, the *V*-tip gradually moved away from the pillar surface. As a result, the elastic strain is expected to increase, which could be the reason for the slight increase of flow stress between "*b*" and "*c*" in Fig. 4e.

There is a hint that cross-transition can occur in bulk materials as well. Cayron found that, in a deformed bulk single crystal magnesium, one $\{01\bar{1}2\}$ twin lamella can have two types of long TB segments: one is parallel with $(0\bar{1}12)$ and the other is parallel with $(01\bar{1}2)$ [26]. He also observed that the orientation in such twin lamella was not uniform: the orientation relationship across the $(0\bar{1}12)$ segment is approximately a $(0\bar{1}12)$ twin relation, and that across $(01\bar{1}2)$ segment is approximately a $(01\bar{1}2)$ twin relation. This phenomenon is similar with the cross-transition observed in the present work. This suggests that cross-transition may occur in bulk scale materials, and may potentially contribute to the formation of $\{10\bar{1}2\}$ TB with irregular morphology in polycrystalline Mg alloys and other hcp metals.

Note that DT cross-transition is fundamentally different with secondary twinning and twin-twin interaction, even though the latter two cases can also change the identity of twin. The secondary twinning is that DT occurs within the primary twin volume. The primary twin volume can even be totally consumed by the secondary twin. However, such phenomenon that a secondary twin forms from the primary twin was not observed in our experiments. For the twin-twin interaction, it usually occurs by one twin impinging on another twin. Such interaction often forms a *T*-shaped morphology, which is different from the *V*-shaped morphology caused by cross-transition. If the two twins share the same $\langle 2\bar{1}\bar{1}0\rangle$ axis, *i.e.* co-zone twin-twin interaction, a low angle tilt grain boundary should be created between the two twins [27,28]. But according to the postmortem characterizations (Fig. 4f and 4g), there is no such low angle grain boundary in both twin and matrix, indicating that no twin-twin interaction occurred in our experiments.

In summary, based on the unique $\{10\bar{1}2\}$ TB structure and the twinning mechanism in hcp metals, we propose that when the performed deformation cannot be accommodated by an existed $\{10\bar{1}2\}$ twin but by its conjugated twin variant, cross-transition will occur to accommodate further deformation, which is then verified by *in-situ* TEM tests on magnesium pillars. Our work implies that a $\{10\bar{1}2\}$ twin in hcp metal is very flexible in response to applied loading, which is expected to affect the twin morphology during deformation.

The authors acknowledge the support provided by National Natural Science Foundation of China (52031011, 51971168, 52022076). We thank Dr. C.W. Guo, Dr. P. Zhang, Dr. Y.B. Qin and D.L. Zhang (Xi'an Jiaotong University) for assistance in sample preparation, FIB and TEM experiments.

Declaration of Competing Interest

The authors declare that they have no known competing financial interests or personal relationships that could have appeared to influence the work reported in this paper.

Supplementary materials

Supplementary material associated with this article can be found, in the online version, at doi:10.1016/j.scriptamat.2021.114231.

References

[1] B.A. Bilby, A.G. Crocker, Proc. R. Soc. Lond. Ser. A Math. Phys. Sci. 288 (1413) (1965) 240 -&.
[2] M.H. Yoo, C.T. Wei, Philos. Mag. 14 (129) (1966) 573 -&.
[3] J.W. Christian, S. Mahajan, Prog. Mater. Sci. 39 (1–2) (1995) 1–157.
[4] Q. Yu, L. Qi, K. Chen, R.K. Mishra, J. Li, A.M. Minor, Nano Lett. 12 (2) (2012) 887–892.
[5] Y.T. Zhu, X.Z. Liao, X.L. Wu, Prog. Mater. Sci. 57 (1) (2012) 1–62.
[6] M.W. Chen, E. Ma, K.J. Hemker, H.W. Sheng, Y.M. Wang, X.M. Cheng, Science 300 (5623) (2003) 1275–1277.
[7] Z.J. Zhang, H.W. Sheng, Z.J. Wang, B. Gludovatz, Z. Zhang, E.P. George, Q. Yu, S.X. Mao, R.O. Ritchie, Nat. Commun. 8 (2017) 8.
[8] Z.J. Wang, Q.J. Li, Y. Li, L.C. Huang, L. Lu, M. Dao, J. Li, E. Ma, S. Suresh, Z.W. Shan, Nat. Commun. 8 (2017) 7.
[9] C.X. Huang, K. Wang, S.D. Wu, Z.F. Zhang, G.Y. Li, S. Li, Acta Mater. 54 (3) (2006) 655–665.
[10] M.R. Barnett, Mater. Sci. Eng. A Struct. Mater. Prop. Microstruct. Process. 464 (1–2) (2007) 1–7.
[11] H. El Kadiri, C.D. Barrett, J. Wang, C.N. Tome, Acta Mater. 85 (2015) 354–361.
[12] X. Liao, W. Jian, J. Nie, Y. Jiang, P. Wu, MRS Bull. 41 (4) (2016) 314–319.
[13] B.Y. Liu, J. Wang, B. Li, L. Lu, X.Y. Zhang, Z.W. Shan, J. Li, C.L. Jia, J. Sun, E. Ma, Nat. Commun. 5 (2014) 6.
[14] J. Tu, X.Y. Zhang, Y. Ren, Q. Sun, Q. Liu, Mater. Charact. 106 (2015) 240–244.
[15] B.Y. Liu, L. Wan, J. Wang, E. Ma, Z.W. Shan, Scr. Mater. 100 (2015) 86–89.
[16] K. Dang, S.J. Wang, M.Y. Gong, R.J. McCabe, J. Wang, L. Capolungo, Acta Mater. 185 (2020) 119–128.
[17] Y. He, B. Li, C.M. Wang, S.X. Mao, Nat. Commun. 11 (1) (2020) 8.
[18] H. El Kadiri, J. Kapil, A.L. Oppedal, L.G. Hector, S.R. Agnew, M. Cherkaoui, S.C. Vogel, Acta Mater. 61 (10) (2013) 3549–3563.
[19] X.Y. Zhang, B. Li, Q. Sun, Scr. Mater. 159 (2019) 133–136.
[20] A. Ostapovets, A. Serra, Review of Non-Classical Features of Deformation Twinning in hcp Metals and Their Description by Disconnection Mechanisms, Metals 10 (9) (2020) 1134, doi:10.3390/met10091134.
[21] J.P. Hirth, J. Wang, C.N. Tome, Prog. Mater. Sci. 83 (2016) 417–471.
[22] M.Y. Gong, J.P. Hirth, Y. Liu, Y. Shen, J. Wang, Mater. Res. Lett. 5 (7) (2017) 449–464.
[23] H.X. Zong, X.D. Ding, T. Lookman, J. Li, J. Sun, E.K. Cerreta, A.P. Escobedo, F.L. Addessio, C.A. Bronkhorst, Phys. Rev. B 89 (22) (2014) 5.
[24] Y. Liu, N. Li, M.A. Kumar, S. Pathak, J. Wang, R.J. McCabe, N.A. Mara, C.N. Tome, Acta Mater. 135 (2017) 411–421.
[25] B.Y. Liu, N. Yang, J. Wang, M. Barnett, Y.C. Xin, D. Wu, R.L. Xin, B. Li, R.L. Narayan, J.F. Nie, J. Li, E. Ma, Z.W. Shan, J. Mater. Sci. Technol. 34 (7) (2018) 1061–1066.
[26] C. Cayron, Mater. Des. 119 (2017) 361–375.
[27] Q. Yu, J. Wang, Y.Y. Jiang, R.J. McCabe, C.N. Tome, Mater. Res. Lett. 2 (2) (2014) 82–88.
[28] B.M. Morrow, R.J. McCabe, E.K. Cerreta, C.N. Tome, Metall. Mater. Trans. A Phys. Metall. Mater. Sci. 45A (13) (2014) 5891–5897.